DNA molecules and configurations in a solid-state nanopore microscope

JIALI LI[1,†], MARC GERSHOW[1], DEREK STEIN[2,‡], ERIC BRANDIN[3] AND J. A. GOLOVCHENKO*[1,2]

[1]Department of Physics, [2]Division of Engineering and Applied Sciences, [3]Department of Molecular and Cellular Biology, Harvard University, Cambridge, Massachusetts 02138, USA

[†]Present address: Department of Physics, University of Arkansas, Fayetteville, Arkansas 72701, USA

[‡]Present address: Department of NanoScience, Delft University of Technology, Lorentzweg 1, 2628 CJ, Delft, The Netherlands

*e-mail: golovchenko@physics.harvard.edu

Published online: 24 August 2003; doi:10.1038/nmat965

A nanometre-scale pore in a solid-state membrane provides a new way of electronically probing the structure of single linear polymers, including those of biological interest in their native environments. Previous work with biological protein pores wide enough to let through and sense single-stranded DNA molecules demonstrates the power of using nanopores, but many future tasks and applications call for a robust solid-state pore whose nanometre-scale dimensions and properties may be selected, as one selects the lenses of a microscope. Here we demonstrate a solid-state nanopore microscope capable of observing individual molecules of double-stranded DNA and their folding behaviour. We discuss extensions of the nanopore microscope concept to alternative probing mechanisms and applications, including the study of molecular structure and sequencing.

Probing, characterizing or manipulating single biopolymers like DNA is often accomplished with the aid of optical methods: for example, observing evanescent field fluorescence of dye molecules[1], deflecting light beams in atomic-force microscopes[2,3] or trapping attached dielectric objects with optical tweezers[4,5]. There has also been remarkable progress at the molecular level in the study of the electrical ionic conduction signals from voltage-biased nanoscale biopores[6,7]. More recently, a voltage bias on an α-haemolysin biopore has been shown to induce charged single-stranded DNA and RNA molecules to translocate through the pore[8–10]. Each translocating molecule blocks the open-pore ionic current, providing an electrical signal that depends on several characteristics of the molecule. This system has limits for studies of biological molecules: the pore is of a fixed size, and its stability and noise characteristics are restricted by chemical, mechanical, electrical and thermal constraints. These difficulties may be overcome with the use of a suitable solid-state nanopore[11]. Here we report a solid-state nanopore 'microscope' capable of electronically characterizing single long-chain polymers such as DNA molecules. We also show the first observation of molecule-induced quantized current blockades that reveal the folding configuration of single molecules as they pass through the nanopore.

At its heart the microscope consists of a voltage-biased nanopore, fabricated in a silicon nitride membrane. The membrane separates two chambers of conducting electrolyte solution. The only electrical conduction path from one chamber to the other passes through the nanopore. To resolve interesting molecular structure, the nanopore dimensions must be small enough to avoid averaging over continuous single-molecule configurations induced by thermal fluctuations and large enough to pass the smallest dimensions of the molecule to be probed. For double-stranded DNA (dsDNA), this means a pore diameter and membrane thickness smaller than the molecule persistence length, 50 nm for dsDNA, and a pore diameter larger than the ~2 nm cross-sectional size of the molecule. The recent discovery of ion-beam sculpting[11] allows structures that meet these criteria to be fabricated with desired nanometre-scale dimensions from solid-state materials such as silicon nitride. A transmission electron micrograph (TEM) of an ion-sculpted 3-nm nanopore in a membrane 5–10 nm

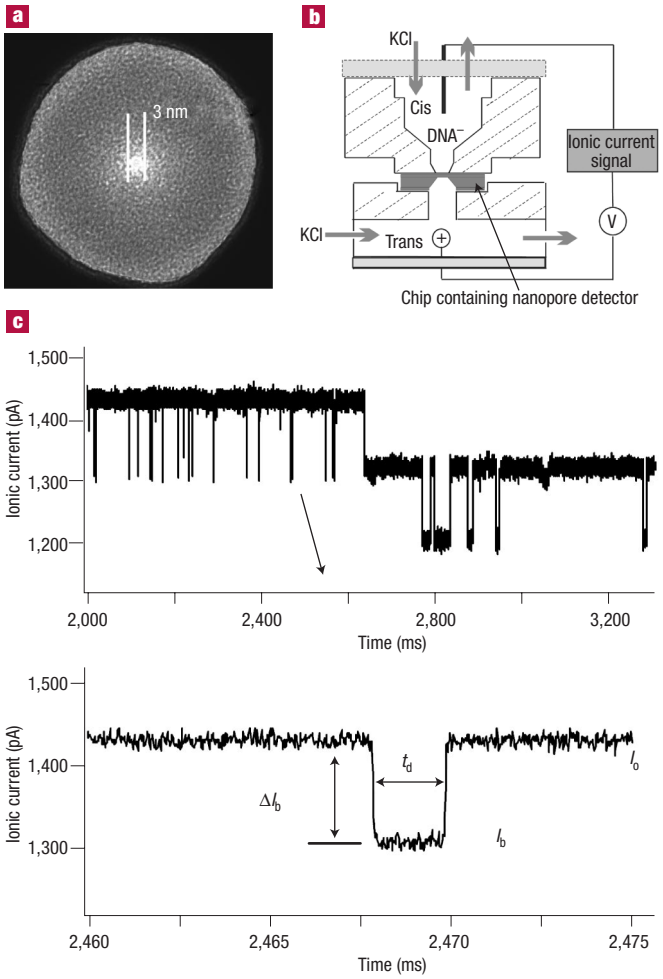

Figure 1 Details of the experimental setup. a, TEM image of a ~3-nm silicon nitride nanopore. **b**, Solid-state nanopore microscope used to obtain electrical signals from single DNA molecules. **c**, Characteristic signals showing transient molecular current blockades and a baseline current shift. Parameters t_d and $<\Delta I_b>$ are shown for a selected simple molecular event.

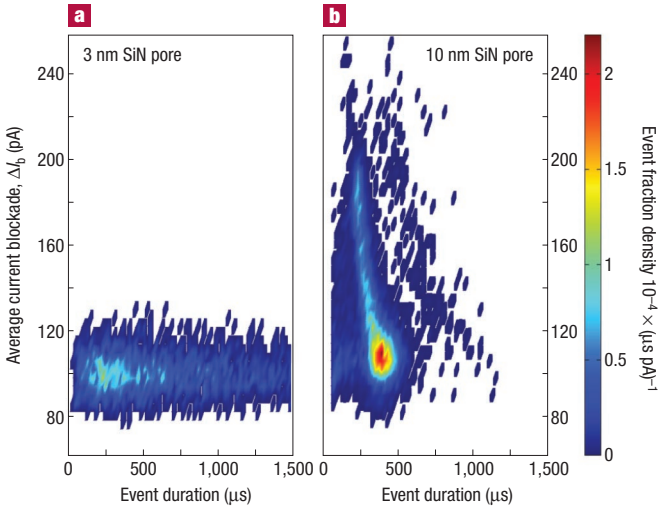

Figure 2 Distribution of events as a function of t_d and $<\Delta I_b>$ for 10-kb dsDNA. **a**, A 3-nm pore, 2,674 events; **b**, a 10-nm pore, 9,477 events. The bias voltage was 120 mV. The colour scale represents event-fraction density normalized as a probability distribution so that the integral of the density over all t_d and $<\Delta I_b>$ is equal to 1.

thick is shown in Fig. 1a, and a schematic of the experimental setup is shown in Fig. 1b.

Open-pore ionic conduction was first established with 120-mV bias across the nanopore. Then DNA was added to the negative *cis* chamber and current blockades appeared in the form of isolated transient reductions in current flow through the pore. Figure 1c shows part of a current trace recorded for 3-kilobase (kb) dsDNA (~1 μm long) and a 3-nm pore. Each event is the result of a single molecular interaction with the nanopore and is characterized by its time duration t_d and its current blockage, ΔI_b, ~120 pA. The expected current blockage from a single molecule blocking the pore is linearly dependent on the cross-sectional area of the molecule and independent of the area of the pore, although because the blockage current varies inversely with the thickness of the pore, different pores may produce different blockage currents for the same molecule. Occasionally, the baseline level shifted for very long periods of time by a magnitude similar to that belonging to a discrete transient molecular event. This was likely due to a single molecule that became 'stuck' in the nanopore. We do not present any molecular data here for time intervals where the open-pore current had been reduced in such a way from its initial value.

Figure 2 shows two plots of the density distribution from many transient molecular events over the parameters $<\Delta I_b>$ and t_d. $<\Delta I_b>$ is defined as the average value of a current blockade over t_d (regardless of the signal's shape). Figure 2a is obtained from experiments using 10-kb dsDNA with a 3-nm pore, and Fig. 2b from experiments with 10-kb dsDNA and a 10-nm pore. The voltage bias across the pore in both cases was 120 mV. The colour coding is keyed to the local density of events normalized by the total number of events for each case. Although both distributions peak at t_d ~ 300–400 μs, the distribution in t_d is quite broad for the 3-nm pore experiment and much sharper for the 10-nm pore experiment. On the other hand, the distribution of events in $<\Delta I_b>$ for the 10-nm pore is much broader than for the 3-nm pore, with larger $<\Delta I_b>$ events showing a definite trend towards having smaller values of t_d.

A visual study of individual events for the 3-nm pore plotted in Fig. 2a shows them all to be simple single-level current blockades of the type at the bottom of Fig. 1c (see also Fig. 4a inset). Approximately 60% of the events in 10-nm pore experiments are of this type, but the remainder are more complex (see Fig. 4b inset). Selecting simple single-level events from the 10-nm-pore data significantly sharpens the distribution in both $<\Delta I_b>$ and t_d. In Fig. 3 we present a histogram of t_d values for simple events in three experiments using 10-nm pores: 3-kb dsDNA with 120-mV bias, 10-kb dsDNA with 120-mV bias, and 10-kb dsDNA with 60-mV bias. The 10-kb dsDNA is seen to take slightly more than three times longer to negotiate the pore than the 3-kb dsDNA at the same bias. Reducing the bias by a factor of two approximately doubles the translocation time. These observations provide strong evidence that each simple single-level event corresponds to a DNA molecule translocating in single-file order through the nanopore under the influence of electrophoretic forces. We shall see that the structure of the more complex signals confirms this interpretation.

Figure 4a shows the density plot of the simple translocation events for 10-kb dsDNA passing through the 10-nm pore. The main cluster of events is narrowly distributed in both $<\Delta I_b>$ and t_d. We shall discuss the second cluster later, but note that its mean $<\Delta I_b>$ is twice that of the main cluster whereas its mean t_d is half. Characteristic time recordings of events from these two regions of the density plot are shown in the inset.

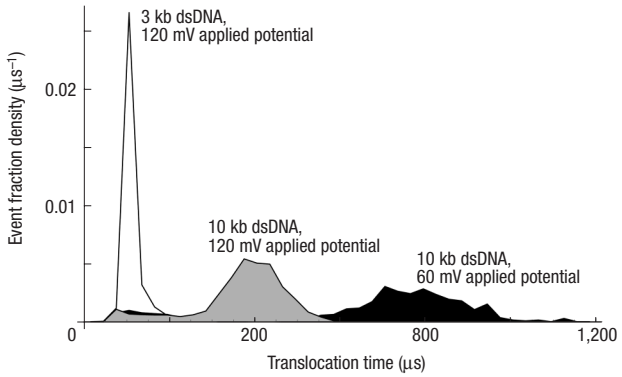

Figure 3 Translocation time distribution function for 3-kb and 10-kb dsDNA molecules in a 10-nm nanopore at 120-mV bias, and for 10-kb dsDNA at 60-mV bias.

Figure 4b shows a density plot for more complex 'multi-level' events that remain after the simple ones are subtracted. Examples of event time recordings in this group are shown in the inset. They look like simple events on which additional blockade structure has been superimposed. For ~85% of the complex events the additional structure appears at the front of the event, ~5% at the rear, 1–2% at both the front and rear, and 5% in the middle. Half of the events with structure in the middle have $t_d > 400$ μs. (More complex structures are also observed in longer t_d events.) We attribute these remarkable additional features to DNA molecules that are folded on themselves as they pass through the pore. As overlapping folded parts of a molecule pass through the pore they enhance the current blockade during that part of the event. If the instantaneous current blockade is proportional to the number of strands of the same molecule in the pore (that is, one or two), one calculates that the average current blockade for the event will be inversely proportional to the translocation time t_d,

$$<\Delta I_b> = <\Delta I_o> t_0/t_d, \quad (1)$$

where $<\Delta I_o>$ and t_0 are the mean current blockage and translocation time of a simple event. This simple model, plotted as the dotted line in Fig. 4b, shows excellent agreement with the data. The smaller cluster in Fig. 4a is thus interpreted as due to molecules that are folded nearly in the middle of the strand. Residual closed-circle plasmid DNA in the sample preparation could presumably contribute to this peak. Events from this second cluster are not included in the simple events plotted in Fig. 3.

More confirmation that complex nanopore signals correspond to events where folded DNA molecules translocate through the pore is provided by a study of the distribution of instantaneous blockade current magnitudes over all events. Assuming the instantaneous

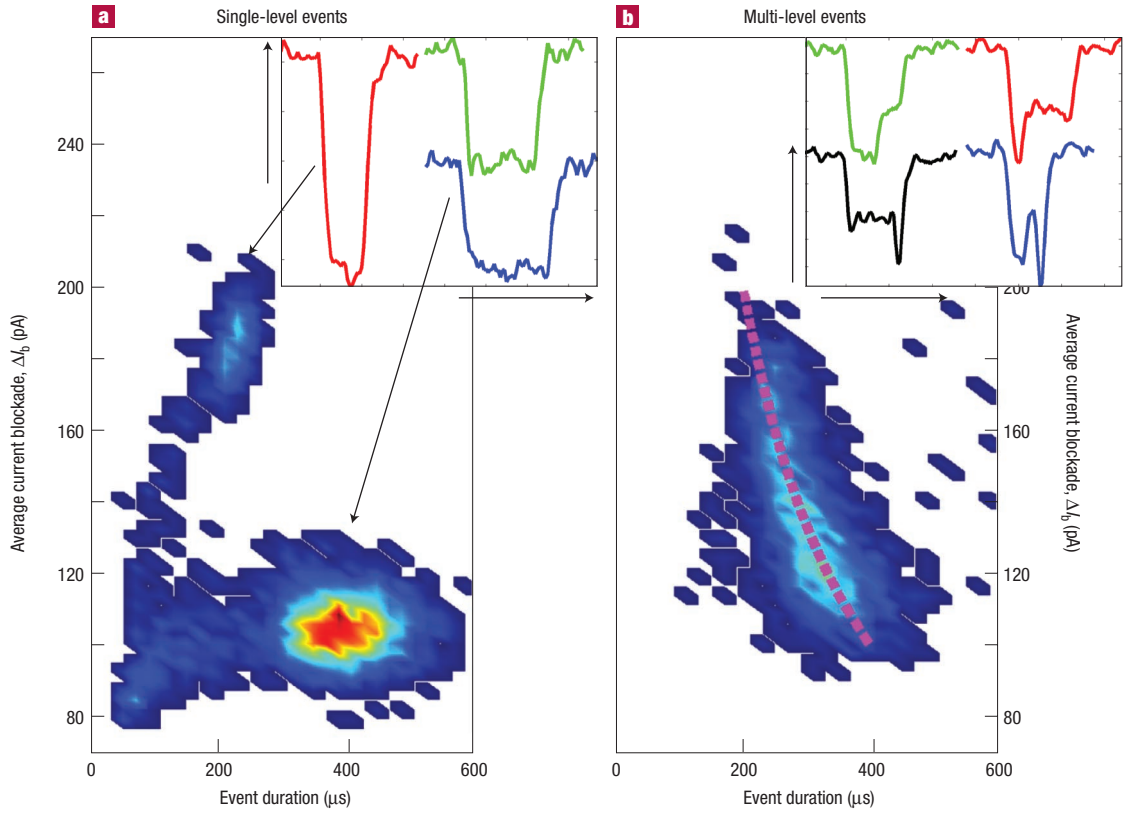

Figure 4 Density of events over t_d and $<\Delta I_b>$ for 10-kb dsDNA passing through a 10-nm pore. a, Simple events characterized by a single blockade level; **b,** the remaining complex events. Inserts show examples of blockade current time traces of events that contribute to the density plots. Isolated regions with only one event in a 20-μs × 2-pA bin are not displayed in this plot. The colour scale is the same as in Fig. 2. The dotted line in **b** represents the prediction of equation (1) in the text with $t_0 = 400$ μs and $<\Delta I_o> = 100$ pA.

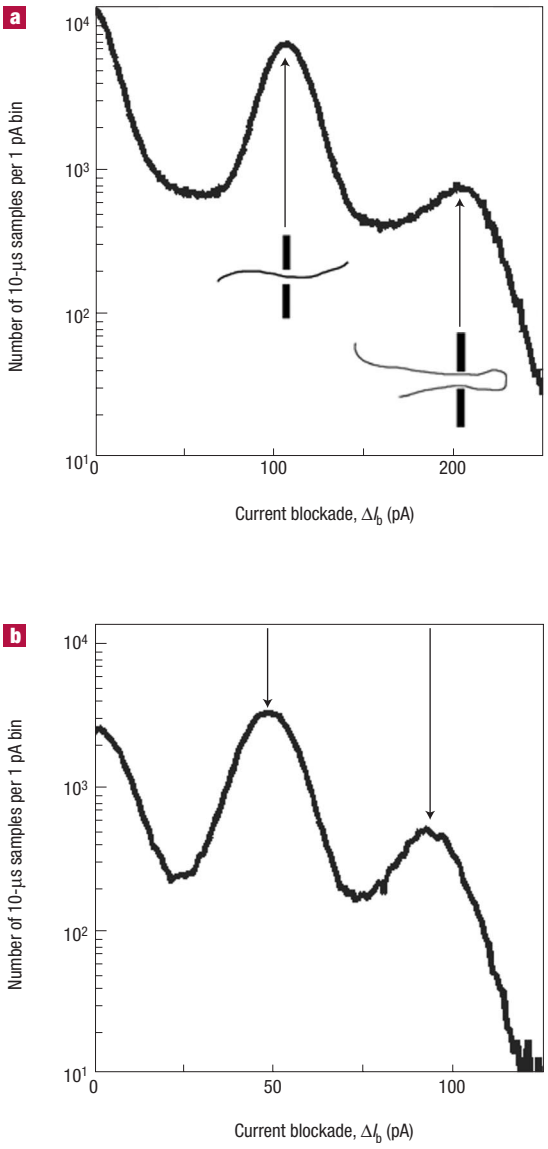

Figure 5 Instantaneous time distribution of blockade current ΔI_b over all events. Current is sampled in a 10-μs time window. The quantized blockade currents corresponding to zero, one and two strands in the pore are clearly seen for 10-kb DNA data from a 10-nm pore for **a**, 120-mV bias and **b**, 60-mV bias.

magnitude of the blocked current is in proportion to the instantaneous number of strands of dsDNA in the nanopore, we expect the distribution of blocked currents taken over many events, in time samples much smaller than an event duration, to show a quantization of local instantaneous ΔI_b values corresponding to zero, one, two, … strands of the folded molecule in the pore at any particular time. A histogram of these sampled values of ΔI_b for 10-μs samples over ~9,500 events (including 200 μs before and after each event) is shown in Fig. 5a for the 10-kb, 120-mV data and in Fig. 5b for the 10-kb, 60-mV data. The expected quantization of sampled ΔI_b values is clearly seen corresponding to zero, one and two molecule strands occupying the nanopore (note the log scale). Experiments with 50-kb DNA and a 15–20-nm pore (data not shown) also show three-level blockades.

A molecular microscope based on solid-state nanopores provides distinct differences from and/or advantages over extant biopore detectors. All results presented here were for dsDNA molecules whose transverse size is ~2 nm. The haemolysin biopore used in previous studies cannot translocate a molecule with such a large diameter[8,12]. We emphasize that because solid-state nanopores can now be fabricated with arbitrary size apertures, the nanopore microscope enables the study of single molecules in a vast category of unlabelled polymers in solution, including RNA, hybridized DNA, and proteins. Furthermore, because of their physical robustness, solid-state nanopores may well be used to study molecules at extremes of temperature, voltage and pH conditions that would destroy biopore-membrane systems.

The average speed of dsDNA molecules translocating through 10-nm pores biased at 120 mV is ~1 cm s^{-1}. A quantitative understanding of this result can involve many complex issues like hydrodynamic interactions and screenings, electro-osmotic flow in and near the pore, and non-equilibrium statistical considerations[13–16]. Here we note that a simple combination of likely relevant parameters, derived by equating the electric force on the charged polymer in the pore to a viscous drag on an effective sphere of radius a on either side of the pore, gives an average translocation speed of

$$v = C\,\frac{\sigma V_{\mathrm{bias}}}{(2a)(6\pi\eta)} \qquad (2)$$

where σ is the linear charge density on the molecule, η the viscosity of the solution, V_{bias} the pore voltage bias, and C is a factor of order unity accounting for the complex issues mentioned above. Setting a to the persistence length of DNA[17] (which implies statistical loss of effective drag force beyond that distance) and assuming a charge of $e/3$ per phosphate, we find that $C \sim 1/2$ brings equation (2) in line with the experimental observations. This crude result suggests that understanding translocation speed may well require only a mesoscopic fluid dynamics description, without the need for invoking strong chemically specific complex interactions between molecule and pore. The agreement also strengthens the notion that the observed signals correspond to molecular translocations.

The observed structured events provide additional compelling evidence in favour of translocation. The quantization of current blockage levels shows that molecules must be completely threading the pore (if molecules were partly blocking the pore, one would expect a continuous range of blockade currents corresponding to different degrees of pore occlusion). The large electric force (8 kT nm^{-1} for 120-mV bias) on a dsDNA molecule in the pore ensures that a molecule that fully enters the pore will translocate. Finally, the fact that deeper blockages correspond to shorter events and the good agreement of the data with equation (1) are consistent only with folded molecules translocating the pore. Although we have previously shown that a solid-state nanopore can be used to detect the presence of DNA molecules[11], these new observations, coupled with the aforementioned length- and bias-dependent measurements, indicate individual molecules translocating the kind of solid-state pore needed for a nanopore microscope.

A new feature of the solid-state nanopore microscope is its ability to detect molecular folding. Most leading-edge folds might be expected to result from a molecule initially encountering the pore at some distance from its end, with the electrophoretic force from the pore forcing a fold as the translocation starts. Simple energetic considerations using the charge on the molecule and its elastic constant show that this is quite possible for the electric fields and pore sizes in our experiments. This does not explain the trailing-edge folds, which we ascribe to the pre-existing state of the molecule (before translocation). The intermediate size 10-nm pore presented here offers a new way of observing this folding. Smaller pores (for example, our 3-nm pore and haemolysin pores) do not allow the passage of a folded molecule, whereas other constrictions recently demonstrated[18,19] are much larger than the

persistence length of DNA, and so do not restrict the passage of DNA to a discrete set of measurable conformations. Figure 2b shows evidence for attractive interactions between different molecules that very occasionally pair up to provide single translocation events for two connected molecules. These appear as a 'ghost' structure at twice the expected translocation times. Although very few, these events form a separate cluster clearly seen in the figure. There are too many of these events to be explained as a simple consequence of the Poisson distribution of event arrivals.

It is important to note that much of our discussion of the solid-state nanopore microscope results has focused on understanding the properties of distributions of molecular events. But that understanding has ultimately enabled us to interpret time histories of individual molecules—and their structures—as they pass through the nanopore in terms of the corresponding highly modulated individual events that are shown in the inset of Fig. 4b. We have thus demonstrated the ability of the solid-state nanopore microscope to resolve multiple features on a single molecule without previous knowledge of the feature's characteristics and to observe new phenomena, like molecular folding and pairing, by means that have not been available in narrower existing biopores. This significantly augments previous work showing that biological pores can distinguish between molecules whose chemical structures[9,20] provide selective binding to a biopore, and work that shows biological pores can trap and sense the spontaneous dissociation of carefully prepared DNA hairpins[21] that are frustrated from translocating the biopore in their associated form. The solid-state pores provide a new way of studying the folding and pairing configurations of single long-chain molecules, the differences between chemically identical molecules in a statistical ensemble, and induced changes in molecular structure that, because of energy restrictions, do not occur naturally in solution.

Finally, we mention that a major advantage of a microscope based on solid-state pores lies in the possibility of articulating the nanopores with electrically conducting electrodes. Such electrodes can allow electronic tunnelling and near-field optical studies of translocating molecules that are linearized and confined in a nanopore of the microscope. Applying these new physical local interactions to molecules translocating through nanopores can provide local single molecule spectroscopies not afforded by measurement of ionic current alone, and offer a means of increasing longitudinal resolution, possibly to the single-base level for DNA, allowing for extremely rapid sequencing of long molecules. It does not seem far-fetched to believe that a mastery of the materials science, surface physics, fluid mechanics, and electrical and optical properties of solid-state nanopores will lead to dramatic improvements in the ability of nanopore microscopes to probe important biological molecules.

METHODS

Nanopores used in our 'microscope' were fabricated in 25 μm × 25 μm free-standing silicon nitride membranes supported by 3 mm × 3 mm × 0.3 mm silicon substrate (100) frames. The 500-nm thick, low-stress (~200 MPa tensile) silicon nitride membrane was deposited by low-pressure chemical vapour deposition. Photolithography and anisotropic wet chemical etching of silicon were used to create the free-standing SiN membrane. An initial 0.1-μm-diameter pore was created at the membrane's centre by using a focused ion beam (Micrion 9500) machine. The diameter of this large pore was then decreased to molecular size near one surface of the membrane by using feedback-controlled ion-beam sculpting[11]. The final nanopore thus resides in a thin 5–10-nm-thick membrane that covers an approximately 0.1-μm-diameter cylindrical aperture that extends through the thick silicon nitride membrane below. Nanopore diameters were determined by transmission electron microscopy (TEM). We note that because the TEM projects a three-dimensional structure onto a two-dimensional plane, the image of the inner edge of the pore actually represents the minimum projected diameter of the pore wall at any height and may not correspond to the narrowest physical constriction. Also, because of the inherent inaccuracies of TEM for determining absolute size and the fact that our pores are not perfectly round, all sizes should be taken as estimates to within a nanometre of the actual pore size.

Figure 1b shows a diagram of the 'nanpore microscope apparatus'. The nanopore on the silicon chip separates two chambers filled with buffered salt solution (1 M KCl, 10 mM TRIS-HCl, pH 8.0). Pre-soaking the chip in isopropanol was found to aid wetting the pore. The *cis* chamber, to which DNA molecules are added, is at the top of the figure and the *trans* chamber at the bottom. Both chambers are made of polydimethylsiloxane and are equipped with AgCl electrodes across which a voltage bias is applied during experiments. The electrode in the *trans* chamber is positively biased and connected to the current-sensing electronics, whereas the other electrode is connected to signal ground.

dsDNA with ~ 3 kb and 10 kb was used in this work. The 3-kb DNA was prepared from pUC19 plasmid (New England Biolabs). The plasmid was cleaved at a single site with *Sma*I restriction enzyme to produce blunt-ended linear dsDNA. The purity and quantity of the recovered DNA after phenol extraction were assessed by agarose gel electrophoresis and ultraviolet absorbance. The 10-kb KBA plasmid[22] was linearized by digestion with the *Sma*I and purified after agarose gel electrophoresis by using the QIAquick gel extraction kit (QIAGEN). The dsDNA was concentrated by ethanol precipitation as described previously[23] and stored dry at 4 °C. Dried dsDNA was suspended in 10 mM Tris, 1 mM EDTA pH 7.6 (RT) before use. Typical concentrations of dsDNA in the *cis* chamber were ~10 nM.

Ionic current through the solid-state nanopore was measured and recorded with an Axopatch 200B integrating patch-clamp amplifier system (Axon Instrument) in resistive feedback mode. Signals were pre-processed by a 10-kHz low-pass filter. Except for the data displayed in Fig. 1c, which are a live recording, all data were acquired in event-driven acquisition mode, meaning analogue start and stop triggers were used to determine when data were to be recorded.

Received 4 April 2003; accepted 27 July 2003; published 24 August 2003.

References

1. Levene, M. J. *et al.* Zero-mode waveguides for single-molecule analysis at high concentrations. *Science* **299,** 682–686 (2003).
2. Rees, W. A., Keller, R. W., Vesenka, J. P., Yang, G. & Bustamante, C. Evidence of DNA bending in transcription complexes imaged by scanning force microscopy. *Science* **260,** 1646–1649 (1993).
3. Hansma, H. G. *et al.* Properties of biomolecules measured from atomic force microscope images: A review. *J. Struct. Biol.* **119,** 99–108 (1997).
4. Quake, S. R., Babcock, H. & Chu, S. The dynamics of partially extended single molecules of DNA. *Nature* **388,** 151–154 (1997).
5. Smith, S. B., Cui, Y. & Bustamante, C. Overstretching b-DNA: The elastic response of individual double-stranded and single-stranded DNA molecules. *Science* **271,** 795–799 (1996).
6. Hille, B. *Ionic Channels and Excitable Membranes* (Sinauer, Sunderland, Massachusetts, 1992).
7. Bezrukov, S. M., Vodyanoy, I. & Parasegian, V. A. Counting polymers moving through a single ion channel. *Nature* **370,** 279–281 (1994).
8. Kasianowicz, J. J., Brandin, E., Branton, D. & Deamer, D. W. Characterization of individual polynucleotide molecules using a membrane channel. *Proc. Natl Acad. Sci. USA* **93,** 13770–13773 (1996).
9. Akeson, M., Branton, D., Kasianowicz, J. J., Brandin, E. & Deamer, D. W. Microsecond time-scale discrimination among polycytidylic acid, polyadenylic acid, and polyuridylic acid as homopolymers or as segments within single RNA molecules. *Biophys. J.* **77,** 3227–3233 (1999).
10. Mellor, A., Nivon, L., Brandin, E., Golovchenko, J. & Branton, D. Rapid nanopore discrimination between single polynucleotide molecules. *Proc. Natl Acad. Sci. USA* **97,** 1079–1084 (2000).
11. Li, J. *et al.* Ion-beam sculpting at nanometre length scales. *Nature* **412,** 166–169 (2001).
12. Sauer-Budge, A. F. *Unzipping Double-Stranded DNA Molecule by Molecule in a Nanopore* Thesis, Harvard Univ. (2002).
13. Muthukumar, M. Dynamics of polyelctrolyte solutions. *J. Chem. Phys.* **107,** 2619–2635 (1997).
14. Muthukumar, M. Polymer translocation through a hole. *J. Chem. Phys.* **111,** 10371–10374 (1999).
15. Muthukumar, M. Polymer escape through a nanopore. *J. Chem. Phys.* **118,** 5174–5184 (2003).
16. Lee, N. & Obukhov, S. Diffusion of a polymer chain through a thin membrane. *J. Physique II* **6,** 195–204 (1996).
17. Evans, D. F. & Wennerström, H. *The Colloidal Domain* 361 (Wiley-VCH, New York, 1999).
18. Han, J. & Craighead, H. G. Separation of long DNA molecules in a microfabricated trap array. *Science* **288,** 1026–1029 (2000).
19. Saleh, O. A. & Sohn, L. L. An artificial nanopore for molecular sensing. *Nano Lett.* **3,** 37–38 (2003).
20. Kasianowicz, J. J., Henrickson, S. E., Weetall H. H. & Robertson, B. Simultaneous multianalyte detection with a nanopore. *Anal. Chem.* **73,** 2268–2272 (2001).
21. Vercoutere, W. *et al.* Rapid discrimination among individual DNA hairpin molecules at single-nucleotide resolution using an ion channel. *Nature Biotechnol.* **19,** 248–252 (2001).
22. Byers, T. J., Husain-Chishti, A., Dubreuil, R. R., Branton, D., & Goldstein, L. S. Sequence similarity of the amino-terminal domain of *Drosophila* β-spectrin to α-actinin and dystrophin. *J. Cell Biol.* **109,** 1633–1641 (1989).
23. Sambrook, J., Fritsch, E. F. & Maniatis, T. *Molecular Cloning: A Laboratory Manual* 2nd edn (Cold Spring Harbor Laboratory, New York, 1989).

Acknowledgements

We acknowledge discussion and criticism of this work by D. Branton, M. Muthukumar and M. Aziz. Dr H. Wang prepared the 3-kb DNA used in the work. A. Kavcic, M. Burns, A. Huang and J. Gu assisted with software analysis. Q. Cai assisted with nanopore preparation and C. Russo provided assistance during preparation of this manuscript. Support for this research has been provided by DARPA, NSF, DOE, AFOSR and Agilent Technologies.
Correspondence and requests for materials should be addressed to J.A.G.

Competing financial interests

The authors declare that they have no competing financial interests.